Anal. Bioanal. Electrochem., Vol. 7, No. 3, 2015, 277-290

Analytical & Bioanalytical Electrochemistry

2015 by CEE
www.abechem.com

Full Paper

Carbon Nanotube/Gold nanoparticles Sensor for Detection of Hydrazine in the Pyrogallol Red Solution

Sathish Reddy,* Ran Du, Hua Xu, Juanxia Wu, Nannan Mao and Jin Zhang[*]

Center for Nanochemistry, Beijing National Laboratory for Molecular Sciences, Key Laboratory for the Physics and Chemistry of Nanodevices, State Key Laboratory for Structural Chemistry of Unstable and Stable Species, College of Chemistry and Molecular Engineering, Peking University, Beijing 100871, China

* Corresponding Author, Tel.: +86-10-6275255; Fax: 86-10-6275-7157

E-Mails: jinzhang@pku.edu.cn (Jin Zhang); gnsathishreddy@gmail.com (Sathish Reddy)

Received: 9 February 2015 / Received in revised form: 30 May 2015 / Accepted: 9 June 2015 / Published online: 30 June 2015

Abstract- An efficient multi-walled carbon nanotube/gold colloidal nanoparticle paste electrode (MWCNTs/ Au Nps PE) was prepared for detection of hydrazine in the presence of pyrogallol red as a mediator in the homogenous solution. The prepared MWCNTs/ Au Nps PE and multi-walled carbon nanotube paste electrode (MWCNTs PE) were characterized by Raman spectroscopy, scanning electron microscopy and cyclic voltammetry. The MWCNTs/ Au Nps PE exhibited a very large decrease in the over potential (0.3V to 0.0V) and significant enhanced peak current response for detection of hydrazine in the presence of pyrogallol red as a mediator in the Na_2CO_3 - KCl solution. The mass transfer of hydrazine on the surface of MWCNTs/Au Nps PE was controlled by adsorption process. The proposed method exhibits outstanding sensitivity (2.5 μA/μM) and low detection limit (0.4 μM) at 0.0V. All the results indicated a good potential application of this sensor in the detection of hydrazine. The use of MWCNTs/ Au Nps PE was demonstrated for detection of hydrazine in the drinking water samples.

Keywords- Gold colloidal nanoparticles, Hydrazine, Multi walled carbon nanotube paste electrode, Cyclic voltammetry, Linear sweep voltammetry

1. INTRODUCTION

Hydrazine (N_2H_4) finds widespread usage in industries, rocket fuel, emulsifiers, catalysts, and weapons of mass destruction, corrosion inhibitors, insecticides and plant growth regulators, etc. [1]. However, hydrazine is threaten to be a toxic chemical for people's health from injection, inhalation of vapors or skin contact produce carcinogenic and mutagenic effects causing severe damage to the liver, lungs, kidneys and human central nervous system [2-5]. Thus, development of a quick and reliable analytical method for the detection of hydrazine is of practical importance. In order to detect hydrazine at low concentrations, various methods, including the spectroscopic [6] methods are available. Among them, an electrochemical technique with a suitable electrode is the most development potential methods because of its fast response, high sensitivity, low cost and reliable [1,7].

It was reported that the hydrazine exhibited irreversible oxidation required large over potential and they have either very low sensitivity or a very high detection limit at conventional available electrodes such as Au, Pt and bare carbon [8-10]. Therefore the literature contains several reports that claim to have solved this problem, The reported approaches includes the use of a nickel ferrite nanoparticles deposited on MWCNTs/ GCE [1], an curcumin- film- coated MWCNTs/ GCE [11], a haematoxlin thin films adsorbed on the MWCNT/GCE [12], an Fe_2O_3 /CP- epoxy composite electrode [13], a reduced graphene sheets/GCE [14] , an Au-SH-SiO_2@ Cu-MoF/GCE [10] and a gold nanoporous particles modified titanium electrode [15]. However, the reported methods have their advantages and limitations in sensitivity, detection limit, over potential and other characteristics. So, it is necessary to have further efforts to fabricate the electrode that can improve the characteristics of electrochemical sensing properties for detection of hydrazine.

Therefore, in order to solve above problems, we have been screened several reported literatures and selected suitable materials for fabrication of the sensor such as; preparation of the electrode by paste method, carbon nanotube as an electrode material, gold nanoparticles as a modifier of the electrode and pyrogallol red as a mediator in the homogenous media. Because in carbon electrodes, especially paste electrodes are widely used in electrochemical investigations [16-18]. Because of their feasibility to incorporate different substances, the easy renewal, the low background currents, composite nature and enhance the electron transfer rate [19]. Due to large edge plane/basal plane ratio of carbon nanotube electrode exhibits rapid electrode kinetics than other carbon electrode. Therefore, CNT-based sensors generally have higher sensitivities and lower limits of detection [20,21]. Moreover, for electroanalytical chemists, more attention has been paid to gold nanoparticles because of their high surface-to-volume ratio, good biological compatibility and excellent conducting capability [22]. Pyrogallol red act as an effective mediator in homogeneous media for enhancing the electron transfer rate [23].

In this work, multi walled carbon nanotube/ gold colloidal nanoparticle paste electrode (MWCNTs/ Au Nps PE) and MWCNTs PE have been prepared. The MWCNTs/ Au Nps PE in the pyrogallol red solution exhibited enhanced surface area of the electrode, remarkable current sensing behavior for the oxidation of hydrazine, good sensitivity and a low detection limit. This was probably due to the amount of exposed edge plane like sites/ basal plane ratio of MWCNTs, surface-to-volume ratio of gold colloidal nanoparticles distributed in the electrode contributes to the immediate conductivity, promoting the electron transfer reaction and pyrogallol red act as an effective homogenous mediator for further enhance the electron transfer rate of the electrode with reduction of oxidation potential of hydrazine [20-23]. The proposed method was successfully applied for the detection of hydrazine concentration in drinking water samples.

2. EXPERIMENTAL PART

2.1. Reagents and chemicals

All analytical grade or high purity chemicals, namely, $K_3[Fe(CN)_6]$ (Xi Long Chemicals Industries), KCl (Beijing Chemicals), Na_2CO_3 (Beijing Chemicals), multi walled carbon nanotubes (MWCNTs) (C Nano Co. LTD), silicon oil (Hang Ping Chemicals Industries), 5 nm gold colloidal nanoparticles (Sigma-Aldrich), pyrogallol red (Alfa chemicals) and hydrazine (N_2H_4) (Sino pharm chemical reagent Co. LTD) were used as received. $K_3[Fe(CN)_6]$, Na_2CO_3, KCl, pyrogallol red and hydrazine (N_2H_4) were prepared by dissolving in Millipore water. All aqueous solutions were prepared using Millipore water.

All electrochemical measurements were conducted on CHI 660 C electrochemical workstation (Chen Hua Instruments Co., Shanghai, China). A conventional three-electrode electrochemical system was used for all the electrochemical experiments, a saturated calomel electrode (SCE) as reference electrode, a platinum wire as counter electrode, the MWCNTs PE and MWCNTs/ Au Nps PE used as a working electrodes (Ø3.0 mm). All potentials in the paper were reported versus SCE. In addition, the solution was purged with high-purity nitrogen for at least 10.0 min prior to each electrochemical measurement. Working electrodes surface were characterized by scanning electron microscopy (SEM; Hitachi S4800 field emission, Japan) and Raman spectroscopy (a Horiba HR800 Raman system. A 100 objective was used to focus laser beam and to collect Raman signal).

2.2. Functionalization of the multi-walled carbon nanotubes

The MWCNTs were initially submitted to a chemical pre-treatment using a 3:1 (v/v) mixture of concentrated sulphuric acid and nitric acid for 12 h at room temperature. After this, the suspension was filtered, the solid was washed with Millipore water until pH 6.5–7.0 and then it was dried at 120 °C for 5 hours [24,25].

2.3. Preparation of the multi walled carbon nanotube paste electrode

The multi walled carbon nanotube-paste electrode (MWCNTs PE) was prepared by taking weight of 0.24 g multi walled carbon nanotube in 0.25 ml silicon oil. This mixture was thoroughly mixed in an agate mortar for about 30 min and packed into the homemade Teflon cavity and polished using soft paper.

2.4. Preparation of multi walled carbon nanotube/Au colloidal nanoparticles paste electrode

The MWCNTs/ Au Nps PE was prepared by taking weight of 0.120 g MWCNTs PE in 9 µl of gold colloidal particles. This mixture was thoroughly mixed in an agate mortar for about 30 min and packed into the homemade Teflon cavity and polished using soft paper.

3. RESULTS AND DISCUSSION

3.1. Characterization of the electrodes

Scanning electron microscopic images of the electrode surface were taken to explore the surface morphology. Fig. 1 (A) shows typical of functionalized pristine MWCNTs are curved and twisted with each other and have very much smooth surfaces. Fig. 1 (B) and (C) SEM images which are observed to have MWCNTs covered with polymeric binder materials (MWCNTsPE) and MWCNTs covered gold colloidal nanoparticles with polymeric binder materials (MWCNTs/ Au Nps PE) respectively, which produces a surface with a wedded aspect [26,27]. The MWCNTs/ Au Nps PE (Fig. 1 (C)) surface have more porous structures as compared with MWCNTsPE (Fig. 1 (B)). Therefore MWCNTs/ Au Nps PE indicates that the electrode with the largest electro-active surface exhibit faster electron transfer rates, suggesting that the surface roughness is directly related to the amount of exposed edge plane-like sites/ basal plane ratio [20,21,28] and the gold colloidal nanoparticles possess surface-to-volume ratio [22].

The Raman spectra of CNTs usually exhibit four characteristic bonds, the tangential stretching G mode (~1500-1600 cm^{-1}), the D mode (~1350 cm^{-1}) and G' mode (~2700 cm^{-1}) [29-31]. Fig. 1 (D) shows Raman spectra of MWCNTsPE (a), MWCNTs (b) and MWCNTs/ Au Nps PE (c) excited at laser 633nm and obtained Raman spectra's shows three Raman resonate modes such as G (~1337cm^{-1}), D (~1590 cm^{-1}) and G' (~2665 cm^{-1}) these Raman resonate modes ranges are matched to the above explained Raman modes and which indicates that electrode samples contains pure MWCNTs. However, Raman spectra of MWCNTs/ Au Nps PE (Fig. 1 (D) (c)) exhibits enhanced Raman spectra intensity as compared with MWCNTsPE and MWCNTs. The obtained results indicate that presence of gold colloidal nanoparticles in MWCNTs/ Au Nps PE [32]. In MWCNTsPE (Fig. 1 (D) (a)) here the

intensity of Raman spectra was decreased due to the presence of only polymeric binder materials (silicone oil) and absence of gold colloidal nanoparticles in the MWCNTsPE which hindrance the enhancement of Raman spectrum signals with respect to the MWCNTs (Fig.1 (D) (b)).

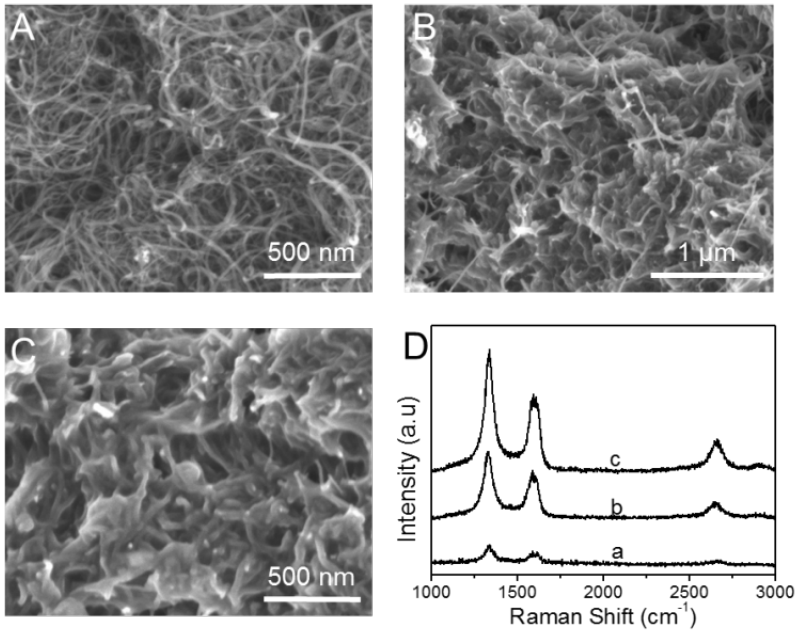

Fig. 1. SEM micrographs of (A) MWCNTs, (B), MWCNTsPE, (C) MWCNTs/ Au Nps PE and (D) Raman spectra's of (a) MWCNTsPE, (b) MWCNTs, (c) MWCNTs/ Au Nps PE

3.2. Electrochemical response and scan rate effects of K_3 [Fe(CN)$_6$]

Fig. 2 (A) shows the cyclic voltammetry response of MWCNTsPE in 1 mM $K_3Fe(CN)_6$ in 1 M KCl at the sweep rate (0.100 Vs^{-1}) exhibits low current signal [ΔEp for MWCNTsPE is 64 mV] as shown in Fig. 2 (A) (a). However, the cyclic voltammetry response is apparently improved at MWCNTs/ Au Nps PE, reflected by the enlargement of the peak currents (ip) [ΔEp for MWCNTs/ Au Nps PE is 64 mV] as shown in Fig. 2 (A) (b). This peak current enhancement shows the strange cyclic voltammograms it is due addition of gold colloidal nanoparticles in the multi walled carbon nanotube paste electrode. The effect of scan rate were studied using cyclic voltammetry for MWCNTsPE and MWCNTs/ Au Nps PE at different sweep rates in 1 mM $K_3Fe(CN)_6$ in a 1 M KCl electrolyte. The obtained graph showed good linearity between the square root of the scan rate ($\upsilon^{1/2}$) and redox peak currents for MWCNTsPE and MWCNTs/Au Nps PE are shown in Fig. 2-(B) & (C). The results of both the electrodes exhibited correlation coefficients of r^2=0.999±0.001. These results indicate that the electron-transfer reaction of MWCNTsPE and MWCNTs/Au Nps PE were a diffusion-controlled process. The surface area of electrode available for the electron transfer to species in the solution can be estimated by the Randles–Sevcik equation (1) [18,33-35].

This equation relates the peak current for an electron-transfer-controlled process with the square root of the scan rate:

$$i_p = 2.69\times10^5\, n^{3/2} A D^{1/2} C \nu^{1/2} \quad (1)$$

Where i_p is the peak current (A), A is the electroactive area (cm^2), C is the concentration of the electroactive species (mol cm^{-3}), n is the number of exchanged electrons, D is the diffusion coefficient ($cm^2\ s^{-1}$) and υ is the scan rate ($V\ s^{-1}$). The value of the diffusion coefficients for K_3 [$Fe(CN)_6$] in KCl solution were obtained from the reported literature [26,36]. The surface area of the MWCNTsPE and MWCNTs/ Au Nps PE was calculated using equation (1) from the slopes of the I_{pa} versus $\nu^{1/2}$ plots are shown in Fig. 2 (B) & (C). The obtained results are found to be 0.064 cm^2 for MWCNTsPE and 0.096 cm^2 for MWCNTs/ Au Nps PE. This results exhibits MWCNTs/Au Nps PE enhanced surface active area as compared with MWCNTsPE. The MWCNTs/Au Nps PE therefore can be used as electrochemical sensors for the investigation of hydrazine.

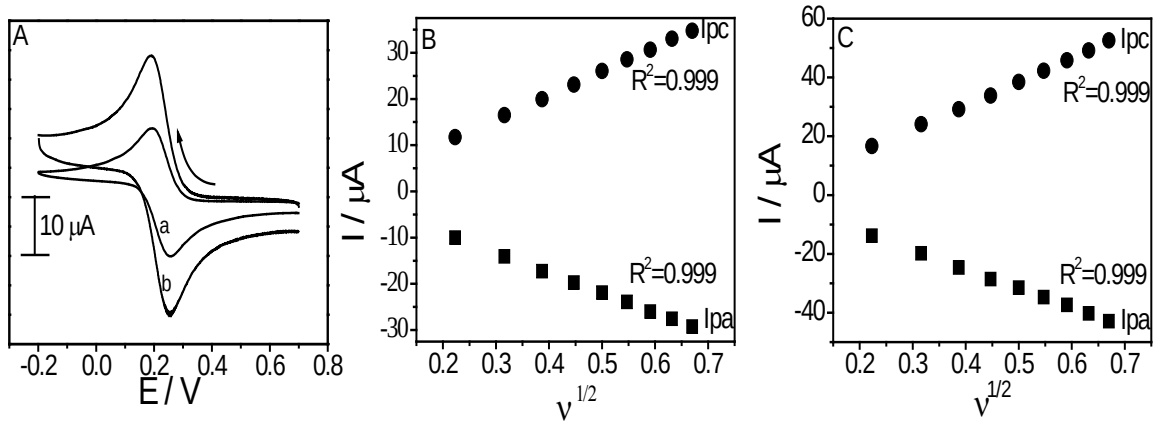

Fig. 2. (A) Cyclic voltammograms of 1 mM $K_3[Fe(CN)_6]$ in 1 M KCl (a) MWCNTsPE, (b) MWCNTs/ Au Nps PE at 0.100 Vs^{-1} and graphs (B &C) shows of redox peak current versus the square root of the scan rate for (B) MWCNTsPE, (C) MWCNTs/ Au NpsPE

3.3. Electrochemical response and scan rate effects of hydrazine

The potential application of MWCNTs/ AuNPs PE sensor was evaluated for electroxidation and detection of hydrazine. In order to study the voltammetric behavior of hydrazine on the surface of prepared electrodes, the cyclic voltammetry was applied for comparison. Fig. 3 (A) depicts the CVs obtained at MWCNTsPE and MWCNTs/ AuNPs PE towards the oxidation of hydrazine. In the absence and presence of 0.5 mM hydrazine in 0.1 M KCl solution at sweep rate (0.100 Vs^{-1}). In the absence of hydrazine there was no electrochemical response {Fig. 3 (A) (a)}. But in the presence of hydrazine there was a well-defined and irreversible oxidation peak for hydrazine at 0.3V. The obtained results indicate

both MWCNTsPE (Fig. 3 (A) (b)) and MWCNTs/ AuNPs PE (Fig. 3 (A) (c)) exhibits good electrocatalytic activity with reduction of background current as compared with the previously reported working electrode such as; bare GCE [1], MWCNTs/GCE [1] , $NiFe_2O_4$ / MWCNTs/ GCE [1], Fe_2O_3/CPE [13], RGS/GCE [14], and Au-SH-SiO_2@Cu-MOF/GCE [15], etc. This was probably due to the MWCNTsPE exposed the number of edge plane like sites/ basal plane ratio and provided high a surface area for contact with hydrazine molecules and increases the electrocatalytic activity of the electrode. In addition, the MWCNTs PE prepared with Au Nps exhibits an excellent electrochemical response for oxidation of hydrazine nearly twice time as compared with the MWCNTsPE. This was probably due to the gold nanoparticles distributed on the exposed edge plane sites/ basal plane ratio of the MWCNTsPE contributes to the immediate electronic conductivity and promoting the electron transfer rate of the electrode (shown in scheme.1) [20-22].

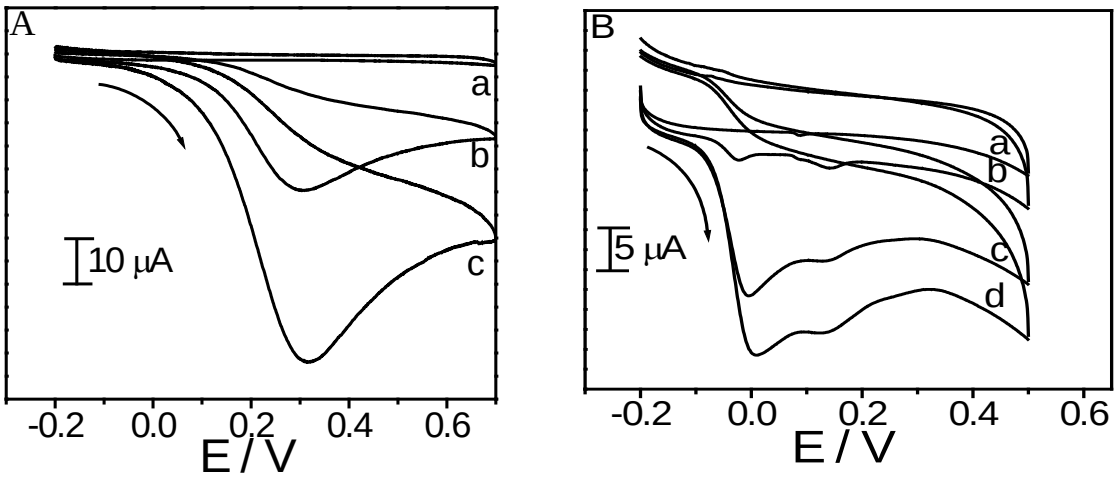

Fig. 3. (A) CVs, in the absence of hydrazine at the MWCNTs/ Au Nps PE (a) and the presence of 0.5 m M hydrazine in 0.1 M KCl at the MWCNTsPE (b) and MWCNTs/ Au Nps PE (c). (B) CVs, in the absence of both hydrazine and pyrogallol red at the MWCNTs/ Au Nps PE (a), in the presence of pyrogallol red and the absence of hydrazine at the MWCNTs/ Au Nps PE (b) and in the presence of 0.2 m M hydrazine in the 0.15 mM pyrogallol red; 0.1 M KCl; 0.01 M Na_2CO_3 solution at the MWCNTsPE (c) and MWCNTs/ Au Nps PE (d)

For electroanalytical chemist, a decrease of over potential for oxidation of hydrazine is very important. Therefore, this work was further improved by using pyrogallol red as a homogenous mediator to enhance the electrocatalytic activity of the MWCNTs/Au Nps PE. Fig. 3 (B) depicts the CVs obtained at MWCNTsPE and MWCNTs/AuNPs PE towards the oxidation of hydrazine in the pyrogallol red solution. In the absence and presence of 0.15 mM pyrogallol red or 0.2 mM hydrazine or both 0.15 mM pyrogallol red and 0.2 mM hydrazine contains in the 0.1 M KCl -0.01 M Na_2CO_3 solution at sweep rate (0.100 Vs^{-1}). In the absence

of both hydrazine and pyrogallol red in electrolyte solution there was no electrochemical response (Fig. 3 (B) (a)) and in the presence of pyrogallol red there was two irreversible oxidation peak as shown in Fig. 3 (B) (b). However, with the addition of hydrazine to the pyrogallol red solutions and the pyrogallol red oxidation peak current increases sharply and the peak potential of pyrogallol red is in lower potential than that of hydrazine. Therefore, pyrogallol red was considered as a suitable homogenous electrocatalyst for reduction of oxidation potential of hydrazine from 0.3 V to 0.0 V at the MWCNTs PE (Fig. 3 (B) (c)) and MWCNTs/ Au Nps PE (Fig. 3 (B) (d)) as a working electrode. The probable mechanism was, in the first step pyrogallol red can be oxidized at the MWCNTs/ Au Nps PE, then in the presence of hydrazine, the oxidized mediator can oxidize hydrazine and converts to its initial form, while the pyrogallol red itself can be further, so the peak current of pyrogallol red increases in the presence of hydrazine [23]. In addition, the prepared MWCNTs/ AuNPs PE exhibits an enhanced peak current response for oxidation of hydrazine in pyrogallol red solution as compared with the MWCNTsPE. This obtained results confirmed that, the gold nanoparticles distributed on the exposed edge plane sites/ basal plane ratio of the MWCNTsPE contributes to the immediate electronic conductivity and simultaneously the pyrogallol red act as a homogenous mediator to promote the electron transfer rate of the electrode (shown in Scheme 1).

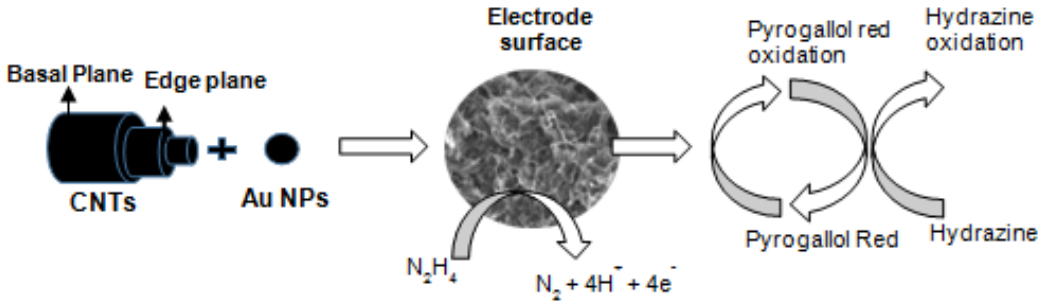

Scheme 1. Schematic diagram showing the mechanism of hydrazine oxidation in pyrogallol red solution at surface of MWCNTs/ Au Nps PE

The scan rate effect for 0.5 mM hydrazine in 0.1 M KCl and 0.2 mM hydrazine in the 0.15 mM pyrogallol red; 0.1 M KCl; 0.01 M Na_2CO_3 solution at the MWCNTs/ Au Nps PE respectively are shown in (Fig. 4 (A) and (B)). As the scan rate increases, the oxidation peak current (I_{pa}) increases. The graph obtained good linear relationship between Ipa and scan rate (υ) was obtained over the range of 0.1-0.45 Vs^{-1} as shown in (Fig. 4 (C) and (D)). Hence, the obtained good linearity between I_{pa} *vs* υ indicate the peak currents responses of the hydrazine on the surface of MWCNTs/ Au Nps PE exhibits adsorption-controlled process.

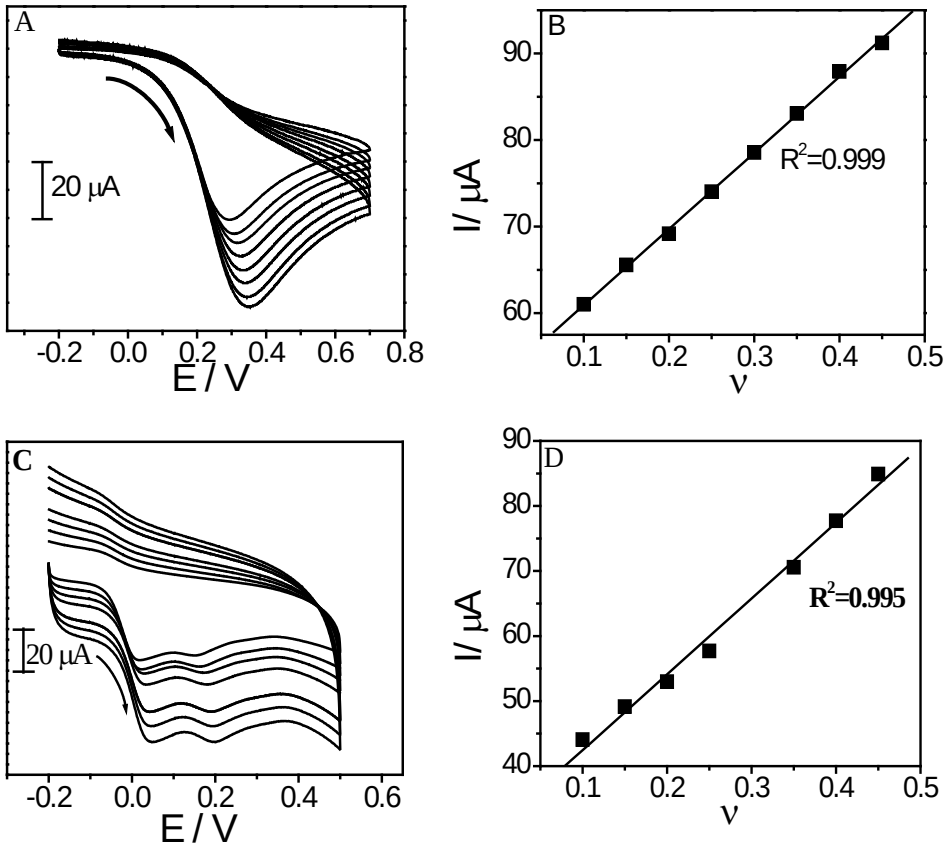

Fig. 4. (A) Cyclic voltammograms of MWCNTs/ Au Nps PE at different scan rates in 0.1 M KCl with 0.5 mM hydrazine. Scan rate: 0.1, 0.15, 0.2, 0.25, 0.3, 0.35, 0.400, 0.45 Vs^{-1} and (B) shows graphs of anodic peak currents (I) versus the scan rate (ν) and Fig. 1 (C) Cyclic voltammograms of MWCNTs/ Au Nps PE at different scan rates in 0.01M Na_2CO_3, 0.15 mM Pyrogallol Red with 0.2 mM hydrazine. Scan rate: 0.1, 0.15, 0.2, 0.25, 0.35, 0.400, 0.45Vs^{-1} and (D) shows graphs of anodic peak currents (I) versus the scan rate (ν)

3.4. The effect of the concentration of hydrazine

The linear sweep voltammetry technique was used for analysis of hydrazine concentration, which was varied from 1.0 to 30 μM. The results at the MWCNTs/ Au Nps PE for the hydrazine concentration analysis in the 0.1 M KCl solution and in the 0.15 mM pyrogallol red; 0.1 M KCl; 0.01 M Na_2CO_3 solution are shown in Figs. 5 (A) and (C), respectively. The corresponding graphs of anodic peak current versus concentration of hydrazine shows linear relationship ranges of 1.0 to 30 μM, with linear regression equations of i_{pa} (μA)=1.029 C hydrazine (μM)+5.185 (μA), (R=0.994) for the hydrazine concentration analysis in the 0.1 M KCl solution at the MWCNTs/ Au Nps PE, as shown in Fig. 5(B). For hydrazine concentrations of 1.0 to 30 μM, the linear regression equations were i_{pa} (μA)=2.5 C hydrazine (μM)–4.383 (μA), (R=0.996), for the hydrazine concentration analysis in the 0.15

mM pyrogallol red; 0.1 M KCl; 0.01 M Na_2CO_3 solution at MWCNTs/ Au Nps PE, as shown in Fig. 5(D).

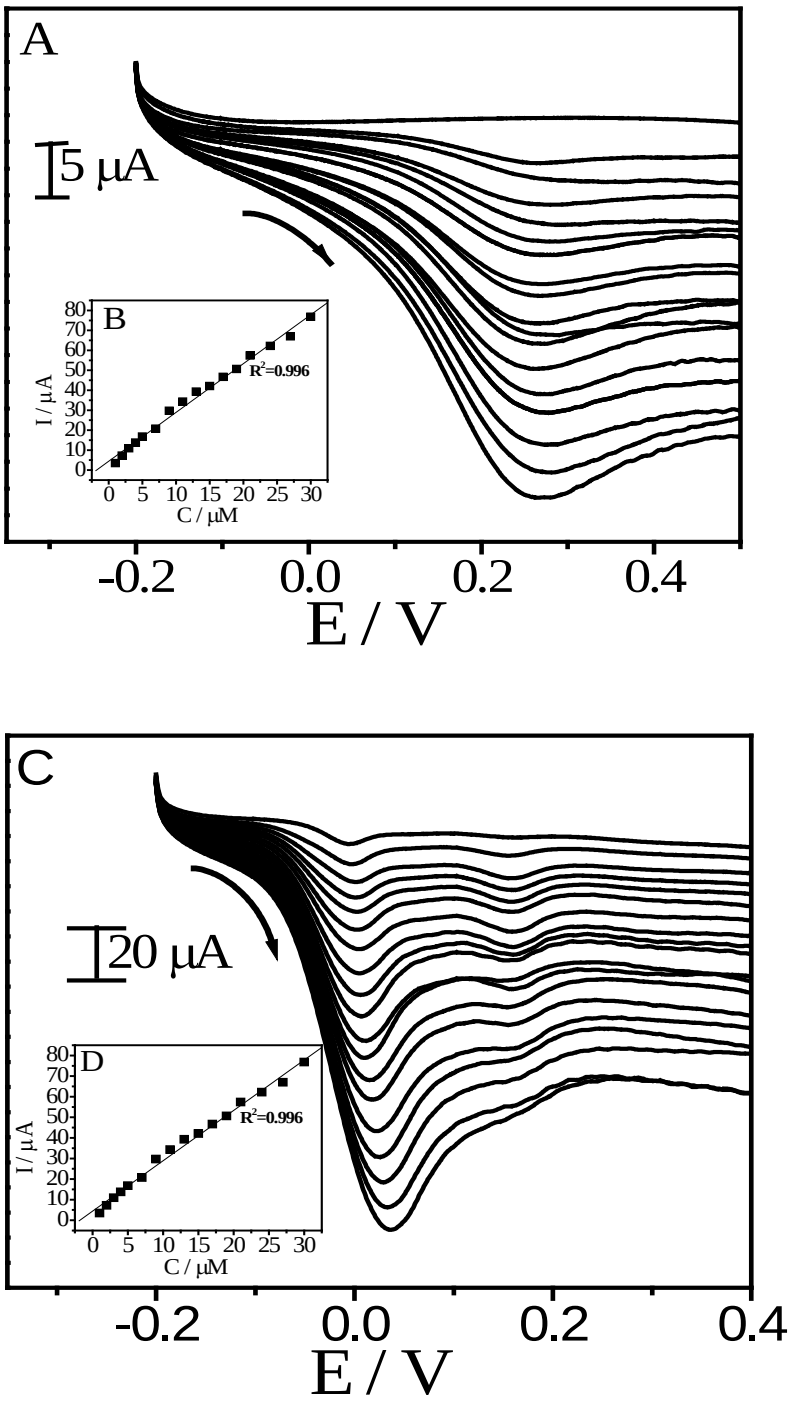

Fig. 5. Linear sweep voltammograms of (1.0 to 30 μM) hydrazine concentrations in 0.1 M KCl at MWCNTs/ Au Nps PE (A), in 0.15 mM pyrogallol red contains in 0.1 M KCl - 0.01 M Na_2CO_3 solution at MWCNTs/ Au NpsPE (C) and shows graph peak current versus concentration of hydrazine (1.0 to 30 μM) in 0.1 M KCl (B) and in the 0.15 mM pyrogallol red; 0.1 M KCl; 0.01 M Na_2CO_3 solution (D) at MWCNTs/ Au NpsPE

The detection limits for hydrazine was 8×10^{-7} M and sensitivity was found to be 1.029 μA/μM in the 0.1 M KCl solution at the MWCNTs/ Au Nps PE. And, in the 0.15 mM pyrogallol red; 0.1 M KCl; 0.01 M Na_2CO_3 solution, the detection limits for hydrazine was 4×10^{-7} M and sensitivity was found to be 2.447 μA/μM at the MWCNTs/ Au Nps PE. The limit of detection (LOD) was calculated according to the equation LOD=K S^0/S, where K is a constant related to the confidence level. In accordance with the suggestion of the IUPAC, the value of K is 3 at the 99% confidence level, S^0 is the standard deviation of ten blank-solution measurements (no added hydrazine), and S is the slope of the calibration graph. The proposed MWCNTs/ Au Nps PE in the 0.15 mM pyrogallol red; 0.1 M KCl; 0.01 M Na_2CO_3 solution exhibited a relatively low oxidation potential for hydrazine, lower detection limit and high sensitivity than those recently reported elsewhere (Table 1) [1,11-15].

3.5. Recovery test for artificial samples

The proposed experimental method here carried for detection of known concentration of hydrazine (by the standard addition method) in a drinking water sample as before and response current obtained was compared with the calibration graph (Fig. 5B & D). The results of the detection of hydrazine were listed in the Table 2 with the hydrazine recovery ranged from 97 to 98.6%.

Table. 1. Comparison of the electrochemical detection of hydrazine at different modified electrode

Electrode	**Ep (V)**	**LOD (μ M)**	**Sensitivity (μA / μM)**	**Reference**
$NiFe_2O_4$/MWCNTs/GCE	0.4	1.5	0.048	[1]
Curcumin/MWCNTs/GCE	0.25	1.4	0.023	[11]
Hematoxylin MWCNTs/GCE	0.23	0.68	0.0208	[12]
Fe_2O_3CP-epoxy composite electrodes	0.8	1.2	0.0445	[13]
Graphene/GCE	0.3	1.0	1.119	[14]
Au Nps /MWCNTsPE	0.3	0.8	1.03	This work
Pyrogallol red /Au Nps /MWCNTsPE	0.0	0. 4	2.50	This work

Table. 2. Results of recovery test

Electrode and solution	Sample (Drinking Water)	Hydrazine added (μM)	Hydrazine found (μM)	Recovery %
MWCNTs/Au Nps PE detection of hydrazine in 0.1 M KCl	01	10	9.90	99
	02	10	9.55	95.5
	03	14	13.55	96.8
	04	18	17.5	97.2
MWCNTs/Au Nps PE detection of hydrazine in 0.1 M KCl , 0.01 M Na_2CO_3 and 0.15 mM Pyrogallol Red	01	8	7.9	98.7
	02	14	13.4	95.7
	03	20	19.8	99
	04	28	27.4	97.8

4. CONCLUSION

In summary, a novel sensor for electrocatalytic oxidation and detection of hydrazine has been described, based on the combination of the MWCNTsPE, Au nanoparticles and pyrogallol red. The proposed method exhibited excellent electrochemical sensing properties with lower detection limit, and high sensitivity for detection of hydrazine as compared with previously reported literatures. Because of the gold nanoparticles distributed on the exposed edge plane sites/ basal plane ratio of the MWCNTsPE contributes to the improved the largest electro-active surface, faster electron transfer rates and simultaneously the pyrogallol red act as a homogenous mediator for further promotes the electron transfer rate of the working electrode.

Acknowledgements

This work was supported by the NSFC (Grants 21233001, 21129001, 51272006 and 51121091) and the MOST (Grant 2011CB932601).

REFERENCES

[1] B. Fang, Y. Feng, M. Liu, G. Wang, X. Zhang, and M. Wang, Microchim. Acta 175 **(**2011) 145.

[2] J. W. Mo, B. Ogorevc, X. Zhang, and B. Pihlar, Electroanalysis 12 (2000) 48.

[3] S. D. Zelnick, D. R. Mattie, and P. C. Stepaniak, Aviat. Space. Environ. Med. 74 (2003) 1285.

[4] S. Garrod, M. E. Bollard, A. W. Nicholls, S. C. Connor, J. Connelly, J. K. Nicholson, and E. Holmes, Chem. Res. Toxicol. 18 **(**2005) 115.
[5] J. Liu, Y. Li, J. Jiang, and X. Huang, Dalton Trans. 39 (2010) 8693.
[6] S. Amlathe, and V. K. Gupta, Analyst 113 (1988) 1481.
[7] W. Sultana, B. Eraiah, and H. N. Vasan, Anal. Method. 4 (2012) 4115.
[8] B. K. Jena, and C. R. Raj, J. Phys. Chem. C 111 **(**2007) 6228.
[9] J. A. Harrison, and Z. A. Khan, J. Electroanal. Chem. 28 **(**1970) 131.
[10] H. Hosseini, H. Ahmar, A. Dehghani, A. Bagheri, A. R. Fakhari, and M. M. Amini, Electrochim. Acta 88 **(**2013) 301.
[11] L. Zheng, and J. Song, Sens. Actuators B 135 **(**2009) 650.
[12] A. Salimi, L. Miranzadeh, and R. Hallaj, Talanta 75 **(**2008) 147.
[13] B. S. ljukic, C. E. Banks, A. Crossley, and R. G. Compton, Electroanalysis 18 **(**2006) 1757.
[14] Y. Wang, Y. Wan, and D. Zhang, Electrochem. Commun. 12 **(**2010) 187.
[15] Q. Yi, and W. Yu, J. Electroanal. Chem. 633 **(**2009) 159.
[16] A. A. Ensafi, M. Lotfi, and H. Karimi-Maleh, Chin. J. Catal. 33 (2012) 487.
[17] S. Anandhakumar, J. Mathiyarasu, and K. L. N. Phani, Anal. Methods. 4 (2012) 2486.
[18] S. Reddy, B. E. K. Swamy, and H. Jayadevappa, Electrochim. Acta 61 **(**2012) 78.
[19] M. D. Rubianes, and G. A. Rivas, Electrochem. Commun. 5 **(**2003) 689.
[20] C. B. Jacobs, M. J. Peairs, and B. J. Venton, Anal. Chim. Acta 662 **(**2010) 105.
[21] C. E. Banks, A. Crossley, C. Salter, S. J. Wilkins, and R. G. Compton, Angew. Chem. Int. Ed. 45 **(**2006) 2533.
[22] S. Guo, and E. Wang, Anal. Chim. Acta 598 **(**2007) 181.
[23] A. A. Ensafi, and E. Mirmomtaz, J. Electroanal.Chem. 583 **(**2005) 176.
[24] B.C. Janegitz, L.H. Marcolino-Junior, S.P. Campana-Filho, R.C. Faria and O. Fatibello-Filho, Sens. Actuators B 142 **(**2009) 260.
[25] A. Afkhami, H. Khoshsafar, H. Bagheri, and T. Madrakian, Mat. Sci. Eng. C 35 (2014) 8.
[26] R. O. Kadara, N. Jenkinson, and C. E. Banks, Sens. Actuators B 138 **(**2009) 556.
[27] M. D. Osborne, B. J. Seddon, R. A.W. Dryfe, G. Lagger, U. Loyall, H. Schafer, and H. H. Girault, J. Electroanal. Chem. 417 **(**1996) 5.
[28] C. E. Banks, T. J. Davies, G. G. Wildgoose, and R. G. Compton, Chem. Commun. 7 (2005) 829.
[29] M. L. Xie, X. C. Yu., Q. C. Feng, J. Zhang, and Z. F. Liu, Acta Phys. Chim. Sin. 26 (2010) 801.
[30] M. S. Dresselhaus, G. Dresselhaus, A. Jorio, A. G. Souza, M. A. Pimenta, and R. Saito, Acc. Chem. Res. 35 **(**2002) 1070.

[31] S. Osswald, M. Havel, and Y. Gogotsi, J. Raman Spectrosc. 38 **(**2007) 728.
[32] L. Liu, T. Wang, J. Li, Z. X. Guo, L. Dai, D. Zhang, and D. Zhu, Chem. Phys. Lett. 367 **(**2003) 728.
[33] K. Saha, S. S. Agasti, C. Kim, X. Li, and V. M. Rotello, Chem. Rev. 112 **(**2012) 2739
[34] D. Salinas-Torresa, F. Huertab, F. Montillaa, and E. Morallona, Electrochim. Acta 56 **(**2011) 2464.
[35] A. J. Bard, and L. R. Faulkner, Electrochemical Methods: Fundamental and Application, Wiley, New York (2000).
[36] R. N. Adams, Electrochemistry at Solid Electrodes, Marcel-Dekker, New York (1969).